J|A|C|S ARTICLES

Published on Web 01/06/2009

# Reduction of a Redox-Active Ligand Drives Switching in a Cu(I) Pseudorotaxane by a Bimolecular Mechanism

Kristy A. McNitt,[†] Kumar Parimal,[†] Andrew I. Share,[†] Albert C. Fahrenbach,[†] Edward H. Witlicki,[†] Maren Pink,[†] D. Kwabena Bediako,[‡] Christina L. Plaisier,[‡] Nga Le,[‡] Lee P. Heeringa,[‡] Douglas A. Vander Griend,[‡] and Amar H. Flood*[,†]

*Department of Chemistry, Indiana University, 800 East Kirkwood Avenue, Bloomington, Indiana 47405, and Department of Chemistry and Biochemistry, Calvin College, Grand Rapids, Michigan 49546*

Received October 31, 2008; E-mail: aflood@indiana.edu

***Abstract:*** The reduction of a redox-active ligand is shown to drive reversible switching of a Cu(I) [2]pseudorotaxane (**[2]PR**$^+$) into the reduced [3]pseudorotaxane (**[3]PR**$^+$) by a bimolecular mechanism. The unreduced pseudorotaxanes **[2]PR**$^+$ and **[3]PR**$^{2+}$ are initially self-assembled from the binucleating ligand, 3,6-bis(5-methyl-2-pyridine)-1,2,4,5-tetrazine (**Me$_2$BPTZ**), and a preformed copper-macrocycle moiety (Cu-**M**$^+$) based on 1,10-phenanthroline. X-ray crystallography revealed a *syn* geometry of the **[3]PR**$^{2+}$. The UV−vis−NIR spectra show low-energy metal-to-ligand charge-transfer transitions that red shift from 808 nm for **[2]PR**$^+$ to 1088 nm for **[3]PR**$^{2+}$. Quantitative analysis of the UV−vis−NIR titration shows the stepwise formation constants to be $K_1 = 8.9 \times 10^8$ M$^{-1}$ and $K_2 = 3.1 \times 10^6$ M$^{-1}$, indicative of negative cooperativity. The cyclic voltammetry (CV) and coulometry of **Me$_2$BPTZ**, **[2]PR**$^+$, and **[3]PR**$^{2+}$ shows the one-electron reductions at $E_{1/2} = -0.96$, $-0.65$, and $-0.285$ V, respectively, to be stabilized in a stepwise manner by each Cu$^+$ ion. CVs of **[2]PR**$^+$ show changes with scan rate consistent with an EC mechanism of supramolecular disproportionation after reduction: **[2]PR**$^0$ + **[2]PR**$^+$ = **[3]PR**$^+$ + **Me$_2$BPTZ**$^0$ ($K_D$*, $k_d$). UV−vis−NIR spectroelectrochemistry was used to confirm the 1:1 product stoichiometry for **[3]PR**$^+$:**Me$_2$BPTZ**. The driving force ($\Delta G_D^* = -5.1$ kcal mol$^{-1}$) for the reaction is based on the enhanced stability of the reduced **[3]PR**$^+$ over reduced **[2]PR**$^0$ by 365 mV (8.4 kcal mol$^{-1}$). Digital simulations of the CVs are consistent with a bimolecular pathway ($k_d = 12\,000$ s$^{-1}$ M$^{-1}$). Confirmation of the mechanism provides a basis to extend this new switching modality to molecular machines.

## Introduction

Redox driven molecular machines[1,2] are being developed as the active materials[3,4] for molecular memory,[5] muscles,[6,7] and electron relays.[8] The functional cores of some of these machines are derived from redox-responsive compounds,[9,10] which often originate in the form of supramolecular complexes.[2] As a consequence, the complexes can be used as a template to synthesize mechanically interlocked structures,[11,12] such as catenanes and rotaxanes. Early successes involved linear motions in $\pi$-donor−acceptor rotaxanes[13] and rotary motions in Cu(I/II) catenates.[14] Recent efforts to enable more sophisticated functions[15,16] have been directed at new and efficient syntheses

[†] Indiana University.

[‡] Calvin College.

(1) (a) Balzani, V.; Credi, A.; Venturi, M. *Molecular Devices and Machines - A Journey into the Nano World*; Wiley-VCH: Weinheim, 2003. (b) Barboiu, M.; Vaughan, G.; Kyritsakas, N.; Lehn, J. M. *Chem.—Eur. J.* **2003**, *9*, 763–769. (c) Flood, A. H.; Ramirez, R. J. A.; Deng, W. Q.; Muller, R. P.; Goddard, W. A.; Stoddart, J. F. *Aust. J. Chem.* **2004**, *57*, 301–322. (d) Sobransingh, D.; Kaifer, A. E. *Org. Lett.* **2006**, *8*, 3247–3250. (e) Champin, B.; Mobian, P.; Sauvage, J.-P. *Chem. Soc. Rev.* **2007**, *36*, 358–366. (f) Lee, J. W.; Hwang, I.; Jeon, W. S.; Ko, Y. H.; Sakamoto, S.; Yamaguchi, K.; Kim, K. *Chem. Asian J.* **2008**, *3*, 1277–1283. (g) Fioravanti, G.; Haraszkiewicz, N.; Kay, E. R.; Mendoza, S. M.; Bruno, C.; Marcaccio, M.; Wiering, P. G.; Paolucci, F.; Rudolf, P.; Brouwer, A. M.; Leigh, D. A. *J. Am. Chem. Soc.* **2008**, *130*, 2593–2601.

(2) Nijhuis, C. A.; Ravoo, B. J.; Huskens, J.; Reinhoudt, D. N. *Coord. Chem. Rev.* **2007**, *251*, 1761–1780.

(3) Kay, E. R.; Leigh, D. A.; Zerbetto, F. *Angew. Chem., Int. Ed.* **2007**, *46*, 72–191.

(4) (a) Ozin, G. A.; Manners, I.; Fournier-Bidoz, S.; Arsenault, A. *Adv. Mater.* **2005**, *17*, 3011–3018. (b) Kinbara, K.; Aida, T. *Chem. Rev.* **2005**, *105*, 1377–1400. (c) Kottas, G. S.; Clarke, L. I.; Horinek, D.; Michl, J. *Chem. Rev.* **2005**, *105*, 1281–1376. (d) Khuong, T. A. V.; Nunez, J. E.; Godinez, C. E.; Garcia-Garibay, M. A. *Acc. Chem. Res.* **2006**, *39*, 413–422. (e) Shirai, Y.; Morin, J. F.; Sasaki, T.; Guerrero, J. M.; Tour, J. M. *Chem. Soc. Rev.* **2006**, *35*, 1043–1055. (f) Paxton, W. F.; Sundararajan, S.; Mallouk, T. E.; Sen, A. *Angew. Chem., Int. Ed.* **2006**, *45*, 5420–5429. (g) Hess, H. *Science* **2006**, *312*, 860–861. (h) Bath, J.; Turberfield, A. J. *Nat. Nanotechnol.* **2007**, *2*, 275–284. (i) Feringa, B. L. *J. Org. Chem.* **2007**, *72*, 6635–6652. (j) Hiraoka, S.; Okuno, E.; Tanaka, T.; Shiro, M.; Shionoya, M. *J. Am. Chem. Soc.* **2008**, *130*, 9089–9098. (k) Hsueh, S. Y.; Cheng, K. W.; Lai, C. C.; Chiu, S. H. *Angew. Chem., Int. Ed.* **2008**, *47*, 4436–4439. (l) Tomasulo, M.; Sortino, S.; Raymo, F. M. *J. Org. Chem.* **2008**, *73*, 118–126.

(5) (a) Collier, C. P.; Mattersteig, G.; Wong, E. W.; Luo, Y.; Beverly, K.; Sampaio, J.; Raymo, F. M.; Stoddart, J. F.; Heath, J. R. *Science* **2000**, *289*, 1172–1175. (b) Flood, A. H.; Stoddart, J. F.; Steuerman, D. W.; Heath, J. R. *Science* **2004**, *306*, 2055–2056. (c) Green, J. E.; Choi, J. W.; Boukai, A.; Bunimovich, Y.; Johnston-Halperin, E.; DeIonno, E.; Luo, Y.; Sheriff, B. A.; Xu, K.; Shin, Y. S.; Tseng, H.-R.; Stoddart, J. F.; Heath, J. R. *Nature* **2007**, *445*, 414–417.

(6) (a) Jimenez-Molero, M. C.; Dietrich-Buchecker, C.; Sauvage, J. P. *Chem.—Eur. J.* **2002**, *8*, 1456–1466. (b) Jimenez-Molero, M. C.; Dietrich-Buchecker, C.; Sauvage, J. P. *Chem. Commun.* **2003**, 1613–1616.

  

of interlocked molecules.[12] This goal also requires and can benefit from complementary efforts aimed at new switching modalities.

Ligand-based switching[17] is an attractive yet less common alternative than that originating from changes in a metal's oxidation state.[9,14,18−20] The reduction of lariat crown ethers to reversibly bind alkali metals was an early precedent[10] that helped establish the fundamentals of redox switching.[2,10] There have been few subsequent extensions. These include oxidation[21] and deprotonation[22] of the ligand as well as some proton-coupled electron transfer reactions[23] and the potentiometric control[24] over ligand tautomers in self-assembled monolayers. Redox-active ligands are also a part of nature's tool box[25] to deal with oxidative stress.[26] The reduced thiol form of cysteine binds Zn(II) ions, while the oxidized disulfide form does not. To the best of our knowledge, however, there are no examples that are designed to employ ligand *reduction* to effect reversible molecular motions[27] within coordination compounds.

***Scheme 1***[a]

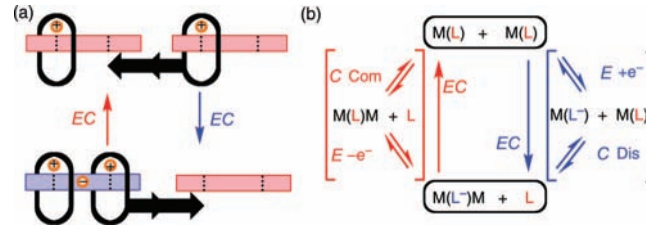


[a] (a) Targeted motions in a supramolecular prototype of a molecular machine and (b) ECEC scheme (after ref 28) representing a cycle of redox chemistry (E) and disproportionation−comproportionation chemistry (C) from 2M(L) to M(L$^-$)M + L that is hypothesized to provide the driving force for switching.

New opportunities can be considered when utilizing ligand reduction. For instance, when the ligand's redox state is responsible for switching instead of the metal's, the metal ion can potentially retain its magnetic, optical, and catalytic functionality irrespective of the switch state. Furthermore, different parameters become available for tuning the switch, such as the $\sigma$-donor, $\pi$-acceptor, and steric properties of the ligand. With these ideas in mind and inspired to elaborate upon a previous report,[28] we are investigating the reduction of redox-active ligands[29] to drive molecular motions (Scheme 1a).

**Design.** Within the realm of coordination chemistry, the reduced anionic form of *N*-heterocyclic ligands can display stronger binding affinities for metal moieties than their electrically neutral counterparts.[30] When such noninnocent ligands[29] are brought together with kinetically labile transition metals, the opportunity to observe chemically reversible switching is

(7) (a) Huang, T. J.; Brough, B.; Ho, C. M.; Liu, Y.; Flood, A. H.; Bonvallet, P. A.; Tseng, H.-R.; Stoddart, J. F.; Baller, M.; Magonov, S. *Appl. Phys. Lett.* **2004**, *85*, 5391–5393. (b) Liu, Y.; Flood, A. H.; Bonvallett, P. A.; Vignon, S. A.; Northrop, B. H.; Tseng, H.-R.; Jeppesen, J. O.; Huang, T. J.; Brough, B.; Baller, M.; Magonov, S.; Solares, S. D.; Goddard, W. A.; Ho, C. M.; Stoddart, J. F. *J. Am. Chem. Soc.* **2005**, *127*, 9745–9759. (c) Wu, J. S.; Leting, K. C. F.; Benitez, D.; Han, J. Y.; Cantrill, S. J.; Fang, L.; Stoddart, J. F. *Angew. Chem., Int. Ed.* **2008**, *47*, 7470–7474.
(8) Katz, E.; Sheeney-Haj-Ichia, L.; Willner, I. *Angew. Chem., Int. Ed.* **2004**, *43*, 3292–3300.
(9) (a) Geiger, W. E. *Prog. Inorg. Chem.* **1985**, *33*, 275–352. (b) Evans, D. H. *Chem. Rev.* **1990**, *90*, 739–751.
(10) (a) Miller, S. R.; Gustowski, D. A.; Chen, Z. H.; Gokel, G. W.; Echegoyen, L.; Kaifer, A. E. *Anal. Chem.* **1988**, *60*, 2021–2024. (b) Boulas, P. L.; Gomez-Kaifer, M.; Echegoyen, L. *Angew. Chem., Int. Ed.* **1998**, *37*, 216–247.
(11) *Molecular Catenanes, Rotaxanes and Knots*; Wiley-VCH: Weinheim, 1999.
(12) (a) Li, Y. J.; Li, H.; Li, Y. L.; Liu, H. B.; Wang, S.; He, X. R.; Wang, N.; Zhu, D. B. *Org. Lett.* **2005**, *7*, 4835–4838. (b) Mobian, P.; Collin, J. P.; Sauvage, J.-P. *Tetrahedron Lett.* **2006**, *47*, 4907–4909. (c) Cabrera, D. G.; Koivisto, B. D.; Leigh, D. A. *Chem. Commun.* **2007**, 4218–4220. (d) Braunschweig, A. B.; Dichtel, W. R.; Miljanic, O. S.; Olson, M. A.; Spruell, J. M.; Khan, S. I.; Heath, J. R.; Stoddart, J. F. *Chem. Asian J.* **2007**, *2*, 634–647. (e) Miljanic, O. S.; Stoddart, J. F. *Proc. Natl. Acad. Sci. U.S.A.* **2007**, *104*, 12966–12970. (f) Nygaard, S.; Laursen, B. W.; Hansen, T. S.; Bond, A. D.; Flood, A. H.; Jeppesen, J. O. *Angew. Chem., Int. Ed.* **2007**, *46*, 6093–6097. (g) Liu, Y.; Klivansky, L. M.; Khan, S. I.; Zhang, X. Y. *Org. Lett.* **2007**, *9*, 2577–2580. (h) Chiu, C. W.; Lai, C. C.; Chiu, S. H. *J. Am. Chem. Soc.* **2007**, *129*, 3500–3501. (i) Fioravanti, G.; Haraszkiewicz, N.; Kay, E. R.; Mendoza, S. M.; Bruno, C.; Marcaccio, M.; Wiering, P. G.; Paolucci, F.; Rudolf, P.; Brouwer, A. M.; Leigh, D. A. *J. Am. Chem. Soc.* **2008**, *130*, 2593–2601. (j) Mullen, K. M.; Gunter, M. J. *J. Org. Chem.* **2008**, *73*, 3336–3350. (k) Koshkakaryan, G.; Parimal, K.; He, J.; Zhang, X.; Abliz, Z.; Flood, A. H.; Liu, Y. *Chem. Eur. J.* **2008**,*14*, 10211−10218.
(13) Bissell, R. A.; Cordova, E.; Kaifer, A. E.; Stoddart, J. F. *Nature* **1994**, *369*, 133–137.
(14) Livoreil, A.; Dietrich-Buchecker, C. O.; Sauvage, J. P. *J. Am. Chem. Soc.* **1994**, *116*, 9399–9400.
(15) Berna, J.; Leigh, D. A.; Lubomska, M.; Mendoza, S. M.; Perez, E. M.; Rudolf, P.; Teobaldi, G.; Zerbetto, F. *Nat. Mater.* **2005**, *4*, 704–710.
(16) (a) Nguyen, T. D.; Tseng, H.-R.; Celestre, P. C.; Flood, A. H.; Liu, Y.; Stoddart, J. F.; Zink, J. I. *Proc. Natl. Acad. Sci. U.S.A.* **2005**, *102*, 10029–10034. (b) Nygaard, S.; Liu, Y.; Stein, P. C.; Flood, A. H.; Jeppesen, J. O. *Adv. Funct. Mater.* **2007**, *17*, 751–762. (c) Angelos, S.; Yang, Y. W.; Patel, K.; Stoddart, J. F.; Zink, J. I. *Angew. Chem., Int. Ed.* **2008**, *47*, 2222–2226.
(17) Allgeier, A. M.; Mirkin, C. A. *Angew. Chem., Int. Ed.* **1998**, *37*, 894–908.
(18) (a) Amendola, V.; Fabbrizzi, L.; Mangano, C.; Pallavicini, P. *Acc. Chem. Res.* **2001**, *34*, 488–493. (b) Fabbrizzi, L.; Foti, F.; Licchelli, M.; Maccarini, P. M.; Sacchi, D.; Zema, M. *Chem.−Eur. J.* **2002**, *8*, 4965–4972. (c) Amendola, V.; Colasson, B.; Fabbrizzi, L.; Douton, M. J. R. *Chem.−Eur. J.* **2007**, *13*, 4988–4997.
(19) (a) Gisselbrecht, J. P.; Gross, M.; Lehn, J. M.; Sauvage, J. P.; Ziessel, R.; Piccinnileopardi, C.; Arrieta, J. M.; Germain, G.; Vanmeerssche, M. *Nou. J. Chim.* **1984**, *8*, 659–667. (b) Collin, J. P.; Gavina, P.; Sauvage, J. P. *New J. Chem.* **1997**, *21*, 525–528. (c) Poleschak, I.; Kern, J. M.; Sauvage, J. P. *Chem. Commun.* **2004**, 474–476. (d) Collin, J. P.; Durola, F.; Mobian, P.; Sauvage, J. P. *Eur. J. Inorg. Chem.* **2007**, *242*, 0–2425. (e) Prikhod'ko, A. I.; Durola, F.; Sauvage, J. P. *J. Am. Chem. Soc.* **2008**, *130*, 448.
(20) (a) Yeh, A.; Scott, N.; Taube, H. *Inorg. Chem.* **1982**, *21*, 2542–2545. (b) Gaudiello, J. G.; Wright, T. C.; Jones, R. A.; Bard, A. J. *J. Am. Chem. Soc.* **1985**, *107*, 888–897. (c) Sano, M.; Taube, H. *J. Am. Chem. Soc.* **1991**, *113*, 2327–2328. (d) Potts, K. T.; Keshavarzk, M.; Tham, F. S.; Raiford, K. A. G.; Arana, C.; Abruña, H. D. *Inorg. Chem.* **1993**, *32*, 5477–5484. (e) Zelikovich, L.; Libman, J.; Shanzer, A. *Nature* **1995**, *374*, 790–792. (f) Zahn, S.; Canary, J. W. *Angew. Chem., Int. Ed.* **1998**, *37*, 305–307. (g) Belle, C.; Pierre, J. L.; Saint-Aman, E. *New J. Chem.* **1998**, *22*, 1399–1402. (h) Li, Y. J.; Huffman, J. C.; Flood, A. H. *Chem. Commun.* **2007**, 2692–2694. (i) Johansson, O.; Lomoth, R. *Inorg. Chem.* **2008**, *47*, 5531–5533.
(21) (a) Desantis, G.; Fabbrizzi, L.; Licchelli, M.; Pallavicini, P.; Perotti, A. *J. Chem. Soc., Dalton Trans.* **1992**, 3283–3284. (b) Liu, X. G.; Eisenberg, A. H.; Stern, C. L.; Mirkin, C. A. *Inorg. Chem.* **2001**, *40*, 2940–2941. (c) Weinberger, D. A.; Higgins, T. B.; Mirkin, C. A.; Stern, C. L.; Liable-Sands, L. M.; Rheingold, A. L. *J. Am. Chem. Soc.* **2001**, *123*, 2503–2516.
(22) Amendola, V.; Fabbrizzi, L.; Mangano, C.; Pallavicini, P.; Perotti, A.; Taglietti, A. *J. Chem. Soc., Dalton Trans.* **2000**, 185–189.
(23) He, Z. C.; Colbran, S. B.; Craig, D. C. *Chem.−Eur. J.* **2003**, *9*, 116–129.
(24) Oklejas, V.; Uibel, R. H.; Horton, R.; Harris, J. M. *Anal. Chem.* **2008**, *80*, 1891–1901.
(25) Maret, W. *Biochemistry* **2004**, *43*, 3301–3309.
(26) Georgiou, G. *Cell* **2002**, *111*, 607–610.
(27) (a) Reduction has been used to affect reactivity; see: (b) Lorkovic, I. M.; Wrighton, M. S.; Davis, W. M. *J. Am. Chem. Soc.* **1994**, *116*, 6220–6228.
(28) (a) Gross, R.; Kaim, W. *Angew. Chem., Int. Ed. Engl.* **1984**, *23*, 614–615. (b) Gross, R.; Kaim, W. *Inorg. Chem.* **1986**, *25*, 498–506.
(29) Ward, M. D.; McCleverty, J. A. *J. Chem. Soc., Dalton Trans.* **2002**, 275–288.
(30) Kaim, W. *Coord. Chem. Rev.* **1987**, *76*, 187–235.

opened up. An early serendipitous example using a noninnocent ligand was observed for a mononuclear complex[28] formed between the manganese(I) metal moiety $\{(\eta^5\text{-}C_5R_5)(CO)_2Mn\}$ and the heterocyclic bridging ligand pyrazine. The dynamic behavior of this system is represented by a redox-centered scheme, or ECEC mechanism (Scheme 1b), for which an electrochemical (E) reduction initiates a chemical (C) process. Initially, reduction of the complex, M(L), generates a formal negative charge localized on the coordinated pyrazine ligand, $M(L^{\bullet-})$. As a consequence, the increased basicity of the uncoordinated nitrogen on the pyrazine drives the formation of the binuclear complex, $M(L^{\bullet-})M$, through disproportionation by reaction with 1 equiv of the unreduced parent complex and, in the process, liberates a free ligand, L. Reoxidation of the binuclear complex, $M(L^{\bullet-})M$, is followed by comproportionation with the free ligand, L, to reform the mononuclear complex, M(L). It should be possible, therefore, to take advantage of noninnocent ligands and labile Cu(I) centers, to drive and facilitate, respectively, intermolecular switching events by ligand reduction.

**Selection of the Components and Their Assembly.** To test this hypothesis a polypyridyl-based thread and macrocycle component were selected as the building blocks to prepare redox-active pseudorotaxanes. The bridging ligand 3,6-bis(5-methyl-2-pyridine)-1,2,4,5-tetrazine (**Me$_2$BPTZ**) was selected as the thread-like noninnocent ligand. It is a dimethylated derivative of the parent BPTZ system,[31] which has been extensively employed in the preparation of mixed-valent compounds[32] and self-assembled into multinuclear structures with a variety of metal ions.[33] In almost all prior examples, the solid state structures of the complexes were found to prefer an *anti* orientation even though there appears to be little preference for either *syn* or *anti* in the free ligand. For the purposes of redox-switching, the ligand displays an accessible reduction[32a] at about −1 V vs Ag/AgCl. Reduction of the coordinated ligand populates a $\pi^*$ orbital that is primarily localized on the tetrazine core.[34] Upon complexation, the reduction shifts increasingly closer to 0 V when the first and second metal moieties are bound.[32a,d−l,35] The concept of switching with a tetrazine derivative was demonstrated recently by using reduction to turn on the binding of a dialkyl thiourea guest.[36]

The ability to use Cu(I)-templated self-assembly to thread binucleating ligands akin to **Me$_2$BPTZ** inside polypyridyl macrocycles has been shown previously in the preparation of heteroligand [*n*]pseudorotaxanes ($n = 2, 3, 4$)[37] and multicomponent architectures.[38] The same preparation strategies[37] have been used herein, and a similar macrocycle (**M**)[39] based on 2,9-diphenyl-1,10-phenanthroline has been selected. The **M** is modified with a benzylic hydroxyl unit for future synthetic modifications. The redox properties of the prior Cu(I) pseudorotaxanes,[37] when using pyridizine in place of tetrazine, were never characterized. However, the redox properties of some related $Cu^I$ grids[40] and of the binuclear $[Cu(PPh_3)_2(\mu\text{-BPTZ})Cu(PPh_3)_2]^{2+}$ complexes[41] have been documented.

This paper is organized into two parts that quantify (1) the stepwise formation of Cu(I) pseudorotaxanes and (2) the mechanism of reduction-induced redox switching of **[2]PR$^+$**. The sequential self-assembly (Scheme 2) of the [2]pseudorotaxane (**[2]PR$^+$**) and the [3]pseudorotaxane (**[3]PR$^{2+}$**) from copper-macrocyle Cu-**M**$^+$ and thread (**Me$_2$BPTZ**) components are verified using electrospray ionization mass spectrometry (ESI-MS) and $^1$H NMR spectroscopy with the *syn* geometry of the **[3]PR$^{2+}$** confirmed from X-ray crystallography. UV−vis−NIR titrations reveal that the **[2]PR$^+$** and **[3]PR$^{2+}$** display some of the lowest metal-to-ligand charge-transfer (MLCT) transitions for a BPTZ complex. These data were used to calculate $K_1$ and $K_2$ values consistent with negative cooperativity. The second


(31) (a) Case, F. H.; Koft, E. *J. Am. Chem. Soc.* **1959**, *81*, 905–906. (b) Dallacker, F. *Monatsh. Chem.* **1960**, *91*, 294–304. (c) Butte, W. A.; Case, F. H. *J. Org. Chem.* **1961**, *26*, 4690–4692. (d) Geldard, J. F.; Lions, F. *J. Org. Chem.* **1965**, *30*, 318–319. (e) Zajac, W. W.; Siuda, J. F.; Nolan, M. J.; Santosus, T. M. *J. Org. Chem.* **1971**, *36*, 3539–3541. (f) Lim, C. L.; Pyo, S. H.; Kim, T. Y.; Yim, E. S.; Han, B. H. *Bull. Korean Chem. Soc.* **1995**, *16*, 374–377. (g) Brown, D.; Muranjan, S.; Jang, Y. C.; Thummel, R. *Org. Lett.* **2002**, *4*, 1253–1256.

(32) (a) Kohlmann, S.; Ernst, S.; Kaim, W. *Angew. Chem., Int. Ed. Engl.* **1985**, *24*, 684–685. (b) Kaim, W.; Ernst, S.; Kohlmann, S.; Welkerling, P. *Chem. Phys. Lett.* **1985**, *118*, 431–434. (c) Jaradat, Q.; Barqawi, K.; Akasheh, T. S. *Inorg. Chim. Acta* **1986**, *116*, 63–73. (d) Kaim, W.; Ernst, S.; Kohlmann, S. *Polyhedron* **1986**, *5*, 445–449. (e) Kaim, W.; Kohlmann, S. *Inorg. Chem.* **1987**, *26*, 68–77. (f) Kaim, W.; Kohlmann, S. *Inorg. Chem.* **1987**, *26*, 1469–1470. (g) Johnson, J. E. B.; de Groff, C.; Ruminski, R. R. *Inorg. Chim. Acta* **1991**, *187*, 73–80. (h) Poppe, J.; Moscherosch, M.; Kaim, W. *Inorg. Chem.* **1993**, *32*, 2640–2643. (i) Roche, S.; Yellowlees, L. J.; Thomas, J. A. *Chem. Commun.* **1998**, 1429–1430. (j) Glockle, M.; Kaim, W.; Katz, N. E.; Posse, M. G.; Cutin, E. H.; Fiedler, J. *Inorg. Chem.* **1999**, *38*, 3270–3274. (k) Chellamma, S.; Lieberman, M. *Inorg. Chem.* **2001**, *40*, 3177–3180. (l) Scheiring, T.; Fiedler, J.; Kaim, W. *Organometallics* **2001**, *20*, 1437–1441. (m) Gordon, K. C.; Burrell, A. K.; Simpson, T. J.; Page, S. E.; Kelso, G.; Polson, M. I. J.; Flood, A. *Eur. J. Inorg. Chem.* **2002**, *55*, 4–563. (n) Ye, S. F.; Kaim, W.; Sarkar, B.; Schwederski, B.; Lissner, F.; Schleid, T.; Duboc-Toia, C.; Fiedler, J. *Inorg. Chem. Commun.* **2003**, *6*, 1196–1200. (o) Sarkar, B.; Kaim, W.; Schleid, T.; Hartenbach, I.; Fiedler, J. *Zeit. Anorg. Allge. Chem.* **2003**, *629*, 1353–1357. (p) Sarkar, B.; Frantz, S.; Kaim, W.; Duboc, C. *Dalton Trans.* **2004**, 3727–3731.

(33) (a) Campos-Fernández, C. S.; Clérac, R.; Dunbar, K. R. *Angew. Chem., Int. Ed.* **1999**, *38*, 3477–3479. (b) Bu, X.-H.; Morishita, H.; Tanaka, K.; Biradha, K.; Furusho, S.; Shionoya, M. *Chem. Commun.* **2000**, 971–972. (c) Campos-Fernandez, C. S.; Clerac, R.; Koomen, J. M.; Russell, D. H.; Dunbar, K. R. *J. Am. Chem. Soc.* **2001**, *123*, 773–774. (d) Constable, E. C.; Housecroft, C. E.; Kariuki, B. M.; Kelly, N.; Smith, C. B. *Inorg. Chem. Commun.* **2002**, *5*, 199–202. (e) Constable, E. C.; Housecroft, C. E.; Kariuki, B. A.; Kelly, N.; Smith, C. B. *Comptes Rendus Chimie* **2002**, *5*, 425–430. (f) Schottel, B. L.; Bacsa, J.; Dunbar, K. R. *Chem. Commun.* **2005**, 46–47l. (g) Campos-Fernandez, C. S.; Schottel, B. L.; Chifotides, H. T.; Bera, J. K.; Bacsa, J.; Koomen, J. M.; Russell, D. H.; Dunbar, K. R. *J. Am. Chem. Soc.* **2005**, *127*, 12909–12923. (h) Schottel, B. L.; Chifotides, H. T.; Shatruk, M.; Chouai, A.; Perez, L. M.; Bacsa, J.; Dunbar, K. R. *J. Am. Chem. Soc.* **2006**, *128*, 5895–5912.

(34) (a) Schwach, M.; Hausen, H. D.; Kaim, W. *Inorg. Chem.* **1999**, *38*, 2242–2243. (b) Remenyi, C.; Reviakine, R.; Kaupp, M. *J. Phys. Chem. A* **2006**, *110*, 4021–4033.

(35) (a) Kaim, W.; Kohlmann, S. *Inorg. Chem.* **1990**, *29*, 2909–2914. (b) Kaim, W.; Kohlmann, S. *Inorg. Chem.* **1986**, *25*, 3306–3310. (c) Garcia Posse, M. E.; Vergara, M. M.; Fagalde, F.; Mellace, M. G.; Katz, N. E. *J. Argn. Chem. Soc.* **2004**, *92*, 101–107.

(36) Jordan, B. J.; Pollier, M. A.; Miller, L. A.; Tiernan, C.; Clavier, G.; Audebert, P.; Rotello, V. M. *Org. Lett.* **2007**, *9*, 2835–2838.

(37) (a) Sleiman, H.; Baxter, P.; Lehn, J.-M.; Rissanen, K. *J. Chem. Soc., Chem. Commun.* **1995**, 715–716. (b) Sleiman, H.; Baxter, P. N. W.; Lehn, J.-M.; Airola, K.; Rissanen, K. *Inorg. Chem.* **1997**, *36*, 4734–4742. (c) Baxter, P. N. W.; Sleiman, H.; Lehn, J.-M.; Rissanen, K. *Angew. Chem., Int. Ed. Engl.* **1997**, *36*, 1294–1296.

(38) (a) Baxter, P. N. W.; Hanan, G. S.; Lehn, J.-M. *Chem. Commun.* **1996**, 2019–2020. (b) Baxter, P. N. W.; Lehn, J.-M.; Fischer, J.; Youinou, M. T. *Angew. Chem., Int. Ed. Engl.* **1994**, *33*, 2284–2287. (c) Baxter, P.; Lehn, J.-M.; Decian, A.; Fischer, J. *Angew. Chem., Int. Ed. Engl.* **1993**, *32*, 69–72. (d) Sleiman, H.; Baxter, P. N. W.; Lehn, J.-M.; Airola, K.; Rissanen, K. *Inorg. Chem.* **1997**, *36*, 4734–4742. (e) Baxter, P. N. W.; Khoury, R. G.; Lehn, J.-M.; Baum, G.; Fenske, D. *Chem.—Eur. J.* **2000**, *6*, 4140–4148.

(39) Jimenez-Molero, M. C.; Dietrich-Buchecker, C.; Sauvage, J.-P. *Chem.—Eur. J.* **2002**, *8*, 1456–1466.

(40) Youinou, M. T.; Rahmouni, N.; Fischer, J.; Osborn, J. A. *Angew. Chem., Int. Ed. Engl.* **1992**, *31*, 733–735.

(41) Schwach, M.; Hausen, H.-D.; Kaim, W. *Inorg. Chem.* **1999**, *38*, 224–2243.

***Scheme 2.*** Stepwise Self-Assembly of Cu-**M**$^+$, **[2]PR**$^+$, and **[3]PR**$^{2+}$ (S = MeCN)[a]

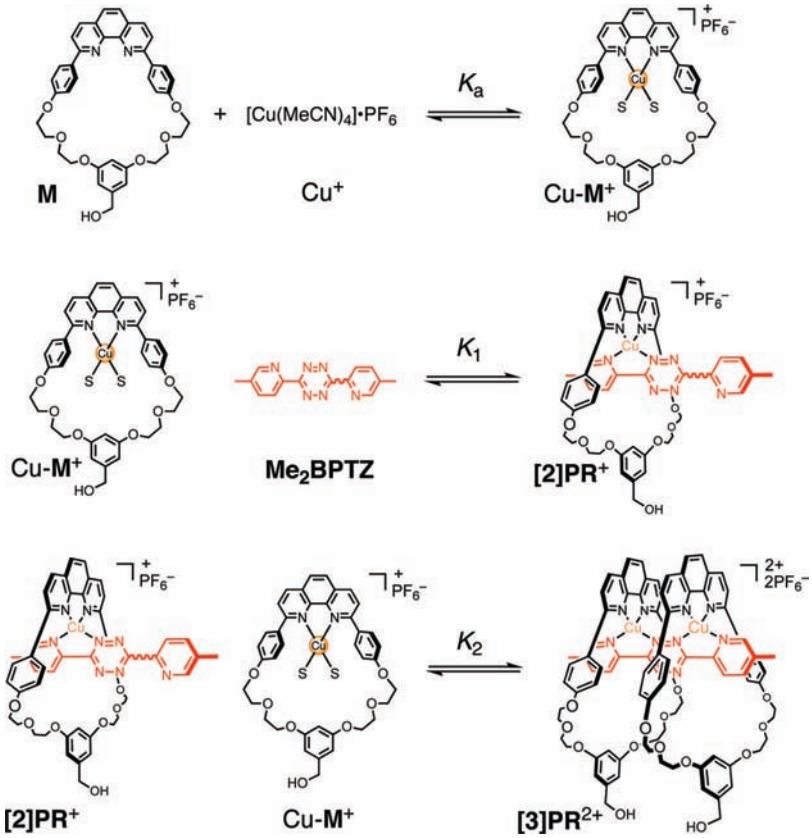


[a] The wavy lines represent *syn-anti* isomerism of **Me$_2$BPTZ**.

part presents the evidence in favor of the reduction-induced switching of a solution of **[2]PR**$^+$. This behavior was confirmed using variable scan-rate cyclic voltammetry (CV) from 50 to 0.2 V s$^{-1}$. The stoichiometry of the products and net chemical reversibility were corroborated using UV−vis−NIR spectroelectrochemistry. The −5.1 kcal mol$^{-1}$ driving force for the reaction was found to stem from the electrostatic stabilization of the reduced ligand by two monocationic Cu$^+$ centers. Lastly, variable concentration CVs in conjunction with digital simulations confirm that switching proceeds by a bimolecular reaction between unreduced **[2]PR**$^+$ and reduced **[2]PR**$^0$.

## Results and Discussion

**Synthesis, Self-Assembly, and Characterization.** The **Me$_2$BPTZ** ligand was synthesized using the known procedures[31,42] for 3,6-disubstituted tetrazines. The macrocycle **M** was prepared from a literature procedure.[39] The equilibria (Scheme 2) can be driven close to completion when the components are mixed in solutions at concentrations that are sufficiently high to ensure tight binding conditions. For each equilibrium, this situation is fulfilled at or above ~1 mM. The copper macrocycle Cu-**M**$^+$ was preformed by mixing equimolar ratios of Cu(MeCN)$_4$•PF$_6$ and **M** in $CH_2Cl_2$ at 4 mM. The self-assembly of the **[2]PR**$^+$ and **[3]PR**$^{2+}$ pseudorotaxanes occurs spontaneously by mixing solutions (~1 mM, $CH_2Cl_2$) of appropriate stoichiometric ratios of Cu-**M**$^+$ and **Me$_2$BPTZ**. For the **[2]PR**$^+$, a darkly tinted purple solution was generated whereas a dark tinted green solution was produced for the **[3]PR**$^{2+}$. The ESI-MS (Figure S1) was utilized to confirm the self-assembly with peaks assigned to the parent ions observed from solutions of the **[2]PR**$^+$ ($M^+$ = 971.6 *m/z*) and **[3]PR**$^{2+}$ ($M^{2+}$ = 839.4 *m/z*). The $^1$H NMR spectra (Figure S2) confirm that the formation of both pseudorotaxanes proceeds in a stepwise manner through the **[2]PR**$^+$ to the **[3]PR**$^{2+}$ in $CD_2Cl_2$ on the basis of the symmetry-dependent methyl groups on the ends of the coordinated **Me$_2$BPTZ** ligand.

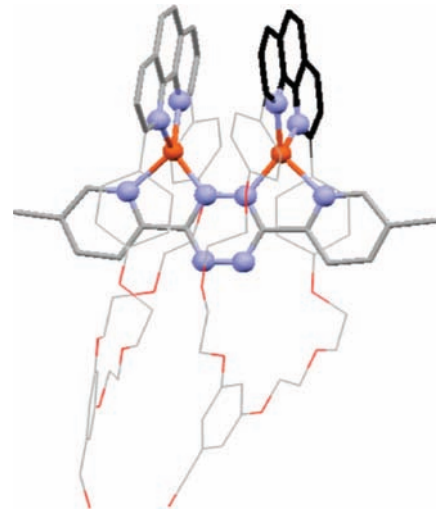

***Figure 1.*** Representation of the *syn* conformation of two coppers in **[3]PR**•2PF$_6$.

**X-ray Crystallographic Analysis of the [3]PR·2PF$_6$.** The crystal structure of the **[3]PR**$^{2+}$ (Figure 1) reveals the *syn*

(42) Abdel-Rahman, M. O.; Kira, M. A.; Tolba, M. N. *Tetrahedron Lett.* **1968**, 3871–3872.

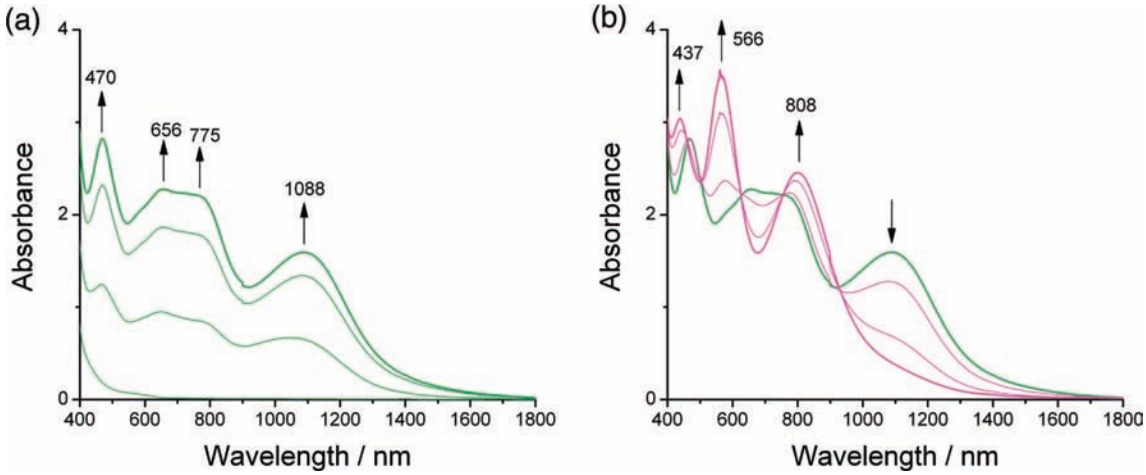


***Figure 2.*** UV−vis−NIR titration following (a) the addition of **Me$_2$BPTZ** (0, 0.2, 0.4, 0.5 equiv) to Cu-**M**$^+$ (1 mM) resulting in the formation of **[3]PR**$^{2+}$ (0.5 mM, green) and (b) after additional aliquots of **Me$_2$BPTZ** (0.5, 0.6, 0.8, 1.0 equiv) converting from **[3]PR**$^{2+}$ to **[2]PR**$^+$ (1 mM, purple).

geometry of the two Cu-**M**$^+$ moieties. This geometry is uncommon for BPTZ complexes, but its presence is explicable from the observations. The parent BPTZ ligand has been crystallized[33,40,41] with a range of metals as both mononuclear and binuclear complexes and ranging from small molecules to extended solid-state networks. The *syn* geometry has only been observed previously for $Ag^+$ binucleated complexes.[33d−h] All of the *anti*-binuclear complexes were formed in the presence of bulky ancillary ligands within octahedral coordination geometries. The $Ag^+$ structures, however, do not contain any other ligands. The tetrahedral-like Cu(I) centers remove the steric effect of ancillary ligands. Considering the parent BPTZ ligand itself, there is an insignificant ∼0.3 kcal mol$^{-1}$ preference (HF/6−31G*) of the *anti* over the *syn* conformation (Supporting Information). The *syn* geometry of **[3]PR**$^{2+}$ is found in conjunction with favorable $\pi-\pi$ slip stacking between phenanthroline units on the two adjacent macrocycles. One of the phenylenes substituted at the 2,9-positions of the phenanthroline-based macrocycles is $\pi$ stacked with the Me$_2$BPTZ thread. The other phenylene is rotated to avoid steric interactions with the neighboring macrocycle. Similar geometrical features were observed in the related pyridazine-based [3]pseudorotaxane,[37] which can only form the *syn* isomer. Therefore, we attribute the preference for the *syn* geometry in **[3]PR**•2PF$_6$ to reduced sterics around the metal and to the presence of $\pi$ stacking that is strong enough to act against both the steric interactions of phenyl rings in the 2,9-positions of the phenanthroline unit and the electrostatic repulsions of neighboring $Cu^+$ ions.

**UV−vis−NIR Spectroscopy and Binding Constant Determination.** The self-assembly of **[2]PR**$^+$ and **[3]PR**$^{2+}$ was monitored using UV−vis−NIR spectroscopy under tight binding conditions by titration (Figure 2) of a concentrated solution of **Me$_2$BPTZ** into a solution of Cu-**M**$^+$. Consistent with the darkly tinted solutions that were observed upon mixing, both pseudorotaxanes absorb across the entire UV−vis region and out into the NIR and they show characteristic bands in their spectra. The **[3]PR**$^{2+}$ shows absorbance peaks of medium intensity at 470 (6800), 656 (4500), 775 (4700), and 1088 (2800) nm (M$^{-1}$ cm$^{-1}$) that grow in upon addition of **Me$_2$BPTZ** up to 0.5 equiv with respect to the 1 equiv of Cu-**M**$^+$ present initially. Further addition of **Me$_2$BPTZ** up to 1 equiv leads to spectroscopic changes that are assigned to the **[2]PR**$^+$ pseudorotaxane with bands growing in at 437 (3500), 566 (4100), and 808 (2800) nm (M$^{-1}$ cm$^{-1}$). The ∼450 nm absorption bands in the spectra of both pseudorotaxanes are assigned to Cu → phenanthroline MLCT transitions.[43] We attribute the red-shifted 470 nm band to the $\pi$ stacking between phenanthroline units. The remaining absorption bands are assigned to Cu → Me$_2$BPTZ MLCT transitions by analogy to related binuclear complexes.[32] The visible absorption band of the **Me$_2$BPTZ** ligand itself, while absorbing at ∼500 nm, is too weak ($\epsilon$ ∼450 M$^{-1}$ cm$^{-1}$) to contribute significantly to the observed spectra. The fact that the lowest-energy electronic transition is red-shifted from 808 nm for **[2]PR**$^+$ to 1088 nm for **[3]PR**$^{2+}$ is consistent with the MLCT assignments: The additional electropositive $Cu^+$ center acts to stabilize the optical acceptor orbital localized on the Me$_2$BPTZ ligand, which is expected[34] to be a tetrazine-localized LUMO.

These MLCT bands are lower in energy compared with most other complexes with the BPTZ ligand. This situation is attributed to a small energy difference ($\Delta E^{redox} = E^{ox} - E^{red}$) between the metal oxidation (Supporting Information) and ligand reduction (*vide infra*) potentials. The redox energy separations for **[2]PR**$^+$ ($\Delta E^{redox}$ = 1.50 V) and **[3]PR**$^{2+}$ ($\Delta E^{redox}$ = 1.40 V) in $CH_2Cl_2$ do not entirely account for the energies of the MLCT bands at 1.53 and 1.14 eV, respectively. The larger discrepancy between the redox and optical energies for the **[3]PR**$^{2+}$ suggests that the electronic configuration of the MLCT excited state [Cu$^{II}$(Me$_2$BPTZ$^-$)Cu$^I$]* is not effectively approximated by the corresponding oxidation states: [Cu$^{II}$(Me$_2$BPTZ)Cu$^I$] and [Cu$^I$(Me$_2$BPTZ$^-$)Cu$^I$]. The kinetically inert binuclear complex [Fe(CN)$_4$($\mu$-BPTZ)Fe(CN)$_4$]$^{4-}$ is the only other example[44] with a low energy MLCT transition showing a shoulder at 1085 nm (1.1 eV, MeCN) and a correspondingly small energy difference between reduction (−0.51 V) and oxidation (+0.35 V) of $\Delta E^{redox}$ = 0.86 eV.

The binding constants $K_a$, $K_1$, and $K_2$ (Scheme 2) were determined from UV−vis−NIR titration data recorded at 50 $\mu$M ($CH_2Cl_2$, 298 K) by using a equilibrium-restricted factor analysis approach[45] (Supporting Information, Section S.6).

(43) Ichinaga, A. K.; Kirchhoff, J. R.; McMillin, D. R.; Dietrich-Buchecker, C. O.; Marnot, P. A.; Sauvage, J.-P. *Inorg. Chem.* **1987**, *26*, 4290–4292.
(44) Glöckle, M.; Kaim, W.; Katz, N. E.; Posse, M. G.; Cutin, E. H.; Fiedler, J. *Inorg. Chem.* **1999**, *38*, 3270–3274.
(45) (a) Vander Griend, D. A.; Bediako, D. K.; DeVries, M. J.; DeJong, N. A.; Heeringa, L. P. *Inorg. Chem.* **2008**, *47*, 656–662. (b) Li, Y.; Vander Griend, D. A.; Flood, A. H. *Supramol. Chem.* **2008**, in press.

Initially, the raw titration data were analyzed using an unrestricted factor analysis to confirm that there are only three absorbing species present in the data set at wavelengths longer than 450 nm, i.e., **Me$_2$BPTZ**, **[2]PR**$^+$, and **[3]PR**$^{2+}$. Modeling of the equilibria in Scheme 2 using HySS[46] verified the importance of including the equilibrium for formation of Cu-**M**$^+$: Cu$^+$ + **M** = Cu-**M**$^+$. This 1:1 association constant was determined in a separate titration (Supporting Information) to be $\Delta G_a = -6.9 \pm 1$ kcal mol$^{-1}$ (298 K, $CH_2Cl_2$). A minimized fit of the titration data for the pseudorotaxanes provided $\Delta G_a = -7.1 \pm 1$, $\Delta G_1 = -12.2 \pm 1.5$ and $\Delta G_2 = -8.9 \pm 0.5$ kcal mol$^{-1}$. The similarity between $\Delta G_a$ values for separate sets of titration data supports the accuracy of the binding constants. These data indicate that the binding of Cu-**M**$^+$ to **Me$_2$BPTZ** operates with negative cooperativity;[47] the ratio $K_1/K_2 = 400$ is much greater than 4. Presumably the $\pi$ stacking in the crystal structure of **[3]PR**$^{2+}$ goes some way toward alleviating any steric and electrostatic repulsions between the two Cu-**M**$^+$ moieties.

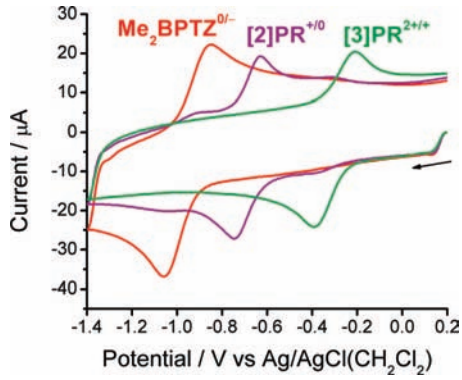


***Figure 3.*** Fast scan-rate (50 V s$^{-1}$) CVs of **Me$_2$BPTZ** (red), **[2]PR**$^+$ (purple), and **[3]PR**$^{2+}$ (green) at 0, 0.9, and 2.0 equiv of Cu-**M**$^+$ added to **Me$_2$BPTZ** at constant concentration: 1 mM was maintained by using Ar bubbling to control the solution volume in $CH_2Cl_2$, glassy carbon, 0.1 M $TBAPF_6$; *iR* compensation was applied.

**Reduction Electrochemistry.** The reduction CVs of **Me$_2$BPTZ**, **[2]PR**$^+$, and **[3]PR**$^{2+}$ (Figure 3) were recorded at fast scan rates (50 V s$^{-1}$) to characterize the half-wave potentials ($E_{1/2}$). These scan rates prevent any reduction-induced switching to occur in the case of **[2]PR**$^+$. The CVs were recorded during a titration of Cu-**M**$^+$ into **Me$_2$BPTZ** showing the stepwise formation of **[2]PR**$^+$ and then **[3]PR**$^{2+}$ (Figure S4) that corresponds closely to the speciation curves calculated using $K_a$, $K_1$, and $K_2$ for this concentration. The reductions are observed at $E_{1/2} = -0.960$, $-0.650$, and $-0.285$ V (vs Ag/AgCl in $CH_2Cl_2$) for **Me$_2$BPTZ**, **[2]PR**$^+$, and **[3]PR**$^{2+}$, respectively. Both **Me$_2$BPTZ** and **[3]PR**$^{2+}$ show one process as a function of scan rate (50 − 0.2 V s$^{-1}$, Figure S5). Coulometry (Table S2) confirms that each reduction is a one-electron process. The peak intensities of **[2]PR**$^+$ and **[3]PR**$^{2+}$ are lower than that of **Me$_2$BPTZ** on account of their lower diffusion coefficients as confirmed by $^1$H NMR analysis (Figure S6). The shifts in $E_{1/2}$ values upon complexation conform to the behavior of kinetically inert BPTZ binuclear complexes.[32d−g,35] The ligand-based reduction, and consequently the LUMO, is stabilized by 310 and 365 mV upon coordination of the first then second monocationic Cu-**M**$^+$ moieties. The stabilization energy is therefore attributed[30] largely to the Coulombic attraction between the tetrazine-localized anion and the monocationic Cu(I) ions.

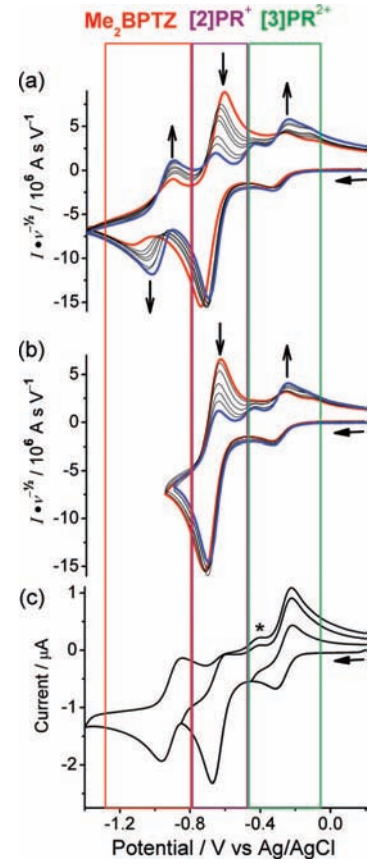


***Figure 4.*** CVs of **[2]PR**$^+$ recorded as a function of decreasing scan rates (see open arrows) for scans down to (a) −1.4 V (25 (red), 10, 7.5, 5, 4, 2, 1.5, and 1 (blue) V s$^{-1}$) and (b) −0.8 V (10 (red), 7.5, 5, 3, 2, 1.5, and 1 (blue) V s$^{-1}$). (c) CVs recorded at 0.2 V s$^{-1}$ with different clipping voltages. Asterisked peak (*) is assigned to the *anti* isomer of **[3]PR**$^+$ (see Supporting Information). Conditions: 1:1 molar mixture of Cu-**M**$^+$:**Me$_2$BPTZ** at 1 mM, 0.1 $TBAPF_6$, Ar degassed $CH_2Cl_2$, Pt counter electrode, for the CVs in (a) and (b). *iR* compensation was used at faster scan rates, and each scan is background subtracted.

**Reduction-Induced Switching of [2]PR**$^+$**.** All of the data presented up to this point provide a basis to examine the evidence in favor of reduction-induced switching in **[2]PR**$^+$. The presence of an EC mechanism stimulated by the reduction of **[2]PR**$^+$ is evident from the variable scan rate CVs. Substantive changes are evident in the CVs when the scan rate is slowed down (Figure 4a and b): (i) A redox couple for the free **Me$_2$BPTZ** grows in at $E_{1/2} = -0.96$ V, (ii) the voltammetric wave for the reoxidation of **[2]PR**$^0$ disappears from the reverse scan, and (iii) the peak for the reduced **[3]PR**$^+$ appears in its place. The other smaller peaks around that for **[3]PR**$^{2+/+}$ are assigned to higher nuclearity species such as grids[40] as well as to the *syn* conformer (Section S.11). These changes indicate that, at 0.2 V s$^{-1}$, the free ligand **Me$_2$BPTZ** and reduced **[3]PR**$^+$ are being generated in reasonable amounts after the reduction of **[2]PR**$^+$ → **[2]PR**$^0$ has occurred. This observation is consistent with the behavior seen for the Mn(I) complex,[28] which undergoes a reduction-induced disproportionation.

To verify that the reduced **[3]PR**$^+$ is generated after reduction of **[2]PR**$^+$, CVs were recorded between different potential windows. When the CV (Figure 4b and c) is "clipped" at −0.85 V just after reduction of **[2]PR**$^+$, it retains the diminished reoxidation

(46) Alderighi, L.; Gans, P.; Ienco, A.; Peters, D.; Sabatini, A.; Vacca, A. *Coord. Chem. Rev.* **1999**, *184*, 311–318.
(47) Badjic, J. D.; Nelson, A.; Cantrill, S. J.; Turnbull, W. B.; Stoddart, J. F. *Acc. Chem. Res.* **2005**, *38*, 723–732.

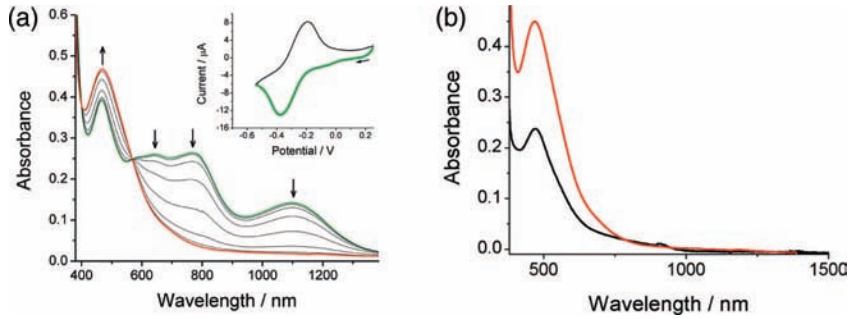


***Figure 5.*** Spectroelectrochemistry of (a) **[3]PR**$^{2+}$ (0.49 mM, 0.1 $TBAPF_6$, $CH_2Cl_2$) showing the spectroscopic changes recorded every 60 mV occurring during the reduction sweep. The inset shows the corresponding CV (0.25 mV $s^{-1}$). (b) Comparison of the spectra for the reduction of solutions containing **[2]PR**$^{+}$ (black) and **[3]PR**$^{2+}$ (red). The intensity of the spectrum for reduced **[2]PR**$^{0}$ is normalized for its concentration (0.6 mM).

peak for **[2]PR**$^0$ and the enhanced reoxidation peak for the reduced **[3]PR**$^+$. When the CV is clipped at −0.45 V, the voltammetric wave for the **[3]PR**$^+$ in the reverse scan was observed to be lower than if the CV was switched at −0.85 V. These results confirm that the production of **[3]PR**$^+$ occurs after reduction of **[2]PR**$^+$. Consistent with this idea, the "inverse" CV (Figure S8), which scans from −0.85 V to positive potentials, shows (a) the same peak heights and potentials as the normal CV (0.2 V $s^{-1}$). (b) When the inverse CV is recorded at 200 V $s^{-1}$ to prevent reformation of **[2]PR**$^+$ by comproportionation at more positive potentials, both voltammetric waves for the **[3]PR**$^{2+/+}$ redox couple are observed. All of these CV experiments confirm that the population of the reduced **[3]PR**$^+$ is increased after the voltammetric wave for reduction of **[2]PR**$^+$.

**UV−vis−NIR Spectroelectrochemistry.** To examine the stoichiometry of the electrochemically driven formation of **[3]PR**$^+$ from **[2]PR**$^+$, spectroelectrochemistry studies were conducted. This technique[48] allows for the simultaneous collection of UV−vis−NIR spectra while executing electrochemistry experiments, thus allowing for the *in situ* visualization of changes in the distribution of molecular species and redox states as reflected by the characteristic absorptions bands. On the basis of Scheme 1, it is predicted that electrolysis of a solution of **[2]PR**$^+$ within the thin layer of the spectroelectrochemistry cell will show the conversion of 1 equiv of **[2]PR**$^+$ into 0.5 equiv of **[3]PR**$^+$ and 0.5 equiv of **Me$_2$BPTZ**.

The spectroelectrochemistry of the **[3]PR**$^{2+}$ system (Figure 5a) was conducted to provide the marker bands of reduced **[3]PR**$^+$. The corresponding thin-layer and slow scan rate CV (0.25 mV $s^{-1}$) displayed one reversible process ($I_c/I_a \sim 1$), and the major spectroscopic changes were observed to follow the onset of Faradaic current. During the reduction, a bleach of the three MLCT bands corresponding to the Cu(I) → $Me_2BPTZ$ transitions were observed simultaneously with an increase in intensity in the band at 470 nm (Figure 5a) assigned to the Cu → phenanthroline MLCT band. The small increase in intensity of the 470 nm band and the absence of any additional transitions in the vis-to-NIR region down to 3200 nm suggests that the coordinated $Me_2BPTZ^{\bullet-}$ ligand anion absorbs light at ~470 nm consistent with related complexes.[32l,m,49] The spectroelectrochemistry of the **Me$_2$BPTZ** ligand alone indicated that the reduced ligand was not stable for the time scale of the experiment. Using the characteristic spectra of **[3]PR**$^+$, the response of the **[2]PR**$^+$ was analyzed by spectroelectrochemistry.

Reduction of a solution containing the **[2]PR**$^+$ (Figure S11) is expected to show absorption bands corresponding to the sum of (a) 0.5 equiv of the reduced **[3]PR**$^+$ species plus (b) 0.5 equiv of the unreduced **Me$_2$BPTZ** ligand. The spectrum generated after reduction of **[2]PR**$^+$ (Figure 5b) coincides with our expectations: The 470 nm band is at half the intensity as it was for reduction of an equimolar solution of **[3]PR**$^{2+}$.

**Thermodynamics of Switching.** The CVs and spectroelectrochemistry are consistent with an ECEC mechanism (Scheme 3).[9,28] Upon reduction ($E_2$) of 0.5 equiv of the **[2]PR**$^+$, a supramolecular disproportionation[50,51] reaction ($K_D$*) takes place between the reduced **[2]PR**$^0$ and neutral **[2]PR**$^+$ forms to generate the reduced **[3]PR**$^+$ pseudorotaxane and free **Me$_2$BPTZ** ligand. Consistent with this idea, both liberated **Me$_2$BPTZ** and reduced **[3]PR**$^+$ were observed in the CVs. During the reverse sweep of the CV, reoxidation ($E_3$) of the **[3]PR**$^+$ species takes place initiating comproportionation ($1/K_D = K_1/K_2$) between the neutral **[3]PR**$^{2+}$ and free **Me$_2$BPTZ** to regenerate the **[2]PR**$^+$ species. We know from binding studies (*vide supra*) that the inequality $K_1 > K_2$ will drive this comproportionation reaction.

The driving force of reduction-induced switching ($K_D$*) can be quantified on the basis of the ladder scheme[9b] (Scheme 4), the known half-wave potentials $E_2$ and $E_3$, and the stepwise formation constants $K_1$ and $K_2$. The reduction-induced switching is represented by a supramolecular disproportionation.

$$\mathbf{[2]PR^+} = \mathbf{Me_2BPTZ} + \mathbf{Cu\text{-}M^+} \qquad 1/K_1 \qquad (1)$$

$$\underline{\mathbf{[2]PR^0} + \mathbf{Cu\text{-}M^+} = \mathbf{[3]PR^+} \qquad K_2^R \qquad (2)}$$

$$\Rightarrow \quad \mathbf{[2]PR^+} + \mathbf{[2]PR^0} = \mathbf{[3]PR^+} + \mathbf{Me_2BPTZ} \qquad K_D^* \qquad (3)$$

The thermodynamic expression for eq 3 can be formulated (Section S.14) as:

$$\Delta G(K_D^*) = F(E_2 - E_3) + \Delta G(K_D) \qquad (4)$$

All of the factors in eq 4 are known and lead to a calculated driving force for the reduction-induced switching reaction of $\Delta G(K_D^*) = -5.1$ kcal $mol^{-1}$.

The thermodynamic description given in eq 4 allows for the driving and restraining forces to be examined. The major driving force, $E_3 - E_2$, is the difference in electrochemical energy (365 mV) between the reduction potentials for **[3]PR**$^{2+/+}$ and **[2]PR**$^{+/0}$. This energy represents the enhanced stabilization of the ligand-localized anion by two monocationic Cu(I) centers

(48) *Spectroelectrochemistry: Theory and Practice*; Gale, R. J., Ed.; Plenum Press: New York, 1988.
(49) Kaim, W.; Berger, S.; Greulich, S.; Reinhardt, R.; Fiedler, J. *J. Organomet. Chem.* **1999**, *582*, 153–159.
(50) Muller, P. *Pure Appl. Chem.* **1994**, *86*, 1077–1184.
(51) The IUPAC identifies more than one definition of disproportionation. The use of supramolecular disproportionation is to distinguish the reaction from the more common relation to changes in oxidation state.

***Scheme 3.*** Electrochemically Driven Switching Cycle of the **[2]PR**$^{+a}$

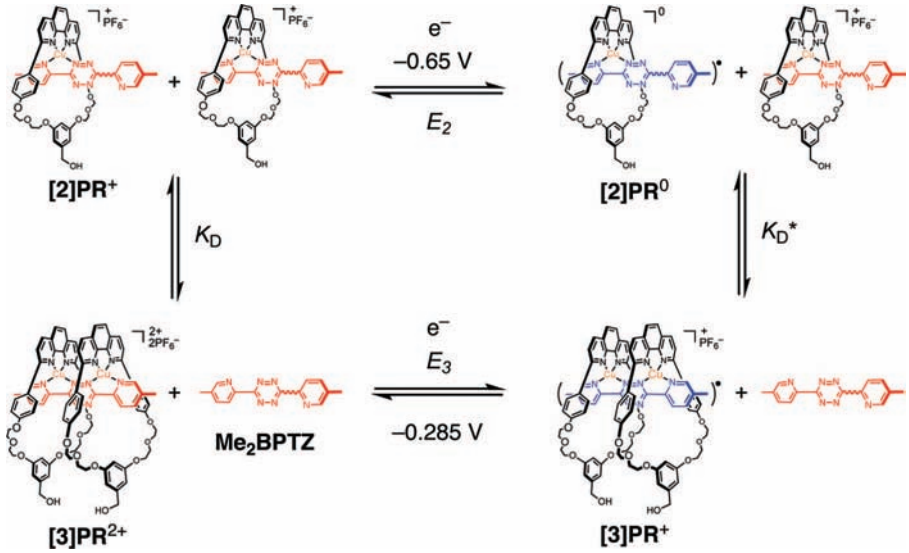


[a] The electrochemistry steps, $E_2$ and $E_3$ refer to reductions of **[2]PR**$^+$ and **[3]PR**$^{2+}$, respectively, and the chemistry steps $K_D$ and $K_D$* refer to disproportionation.

***Scheme 4.*** Electrochemical and Chemical Equilibria Characterizing the Voltammetric Response of **[2]PR**$^+$

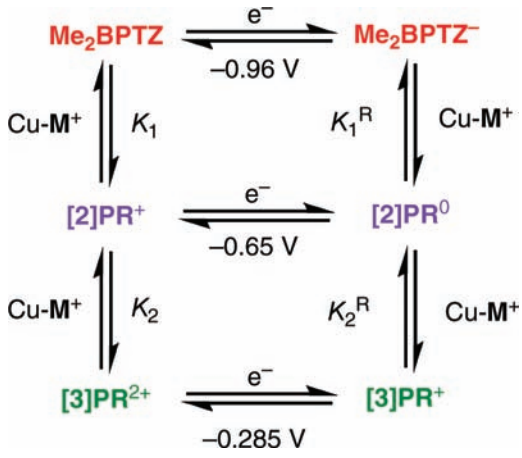


rather than just one and corresponds to 8.4 kcal mol$^{-1}$. In opposition to this is the energy cost involved in the disproportionation reaction in the neutral state ($K_D$) of 3.3 kcal mol$^{-1}$, which is characteristic of negative cooperativity.

**Kinetics and Mechanism of Switching.** Digital simulations (Figure 6 and Section S.15) of the variable scan rate and variable concentration (3.8, 1.9. 0.95, 0.48, and 0.24 mM) CV data were conducted to characterize the mechanism of switching. The CVs were simulated assuming two limiting cases for the supramolecular disproportionation: either a dissociation−association or bimolecular mechanism (Scheme 5). The known values for $E_2$, $K_1$, $K_2^R$, and $K_D$* were used in the simulations. The higher nuclearity species surrounding **[3]PR**$^+$ were not included in the simulations.

For switching when a dissociation−association mechanism (eqs 5−7) was assumed, it was possible to use a common set of parameters to simulate the CV for a given concentration. However, these parameters failed to account for the effect of concentration on the CVs: It was found that the shape of the simulated CVs did not change with concentration (Figure 6b).

***Scheme 5.*** Two Mechanistic Pathways for Electrochemical Switching from the **[2]PR**$^+$

| | | | |
|---|---|---|---|
| Charge Transfer: | **[2]PR**$^+$ + e$^-$ → **[2]PR**$^0$ | $E_2$ ($K_{E2}$) | (5) |
| Dissociation: | **[2]PR**$^+$ → Cu-**M**$^+$ + **Me$_2$BPTZ** | $1/K_1$, $k_1$ | (6) |
| Association: | **[2]PR**$^0$ + Cu-**M**$^+$ → **[3]PR**$^+$ | $K_2^R$, $k_2$ | (7) |
| Bimolecular Pathway: | **[2]PR**$^+$ + **[2]PR**$^0$ → **[3]PR**$^+$ + **Me$_2$BPTZ** | $K_D$*, $k_d$ | (8) |

Simulation of the switching assuming a bimolecular mechanism (eqs 5 and 8) gave rise to a more satisfactory reproduction of the experimental data for all concentrations (Figure 6c).[52] Therefore, the switching proceeds through a bimolecular pathway with a second-order rate constant, $k_d = 12\,000$ s$^{-1}$ M$^{-1}$. The overall rate of switching is governed by the rate law:

$$\text{Rate} = (K_{E2})k_d[\mathbf{[2]PR}^+]^2 \quad (9)$$

This form of the rate law has two implications. First, assuming a diffusion-limited bimolecular rate constant of $\sim 10^9$ M$^{-1}$ s$^{-1}$, only 1 in every 100 000 collisions is successful. This situation is consistent with the need to break Cu−N metal−ligand bonds and to attain an appropriate orientation for a successful reaction. Second, the rate depends upon the position of equilibrium ($K_{E2}$) for the charge-transfer reaction eq 5. For an electrochemical reaction, where the electrode is a reservoir of electrons, a maximum rate of switching can be attained when the applied potential ($E_{ap}$) is equal to $E_2$ such that $K_E = 1$ and there will be equal concentrations of unreduced **[2]PR**$^+$ to react with reduced

(52) Two additional mechanisms were inspected. (a) A solvent assisted pathway stemming from the MeCN introduced into the solution from the $[Cu(MeCN)_4]PF_6$ salt. CVs obtained from solutions with up to 400 equiv of MeCN in $CH_2Cl_2$ (2.5% *v*/*v*) were not adequately simulated using a common set of parameters for the solvent-assisted pathway. Furthermore, physically meaningless rate constants of $k > 10^{11}$ M$^{-1}$ s$^{-1}$, were required. (b) A bimolecular pathway via 2**[2]PR**$^0$ = **[3]PR**$^+$ + **Me$_2$BPTZ**$^-$, was not able to reproduce the experimental CVs.

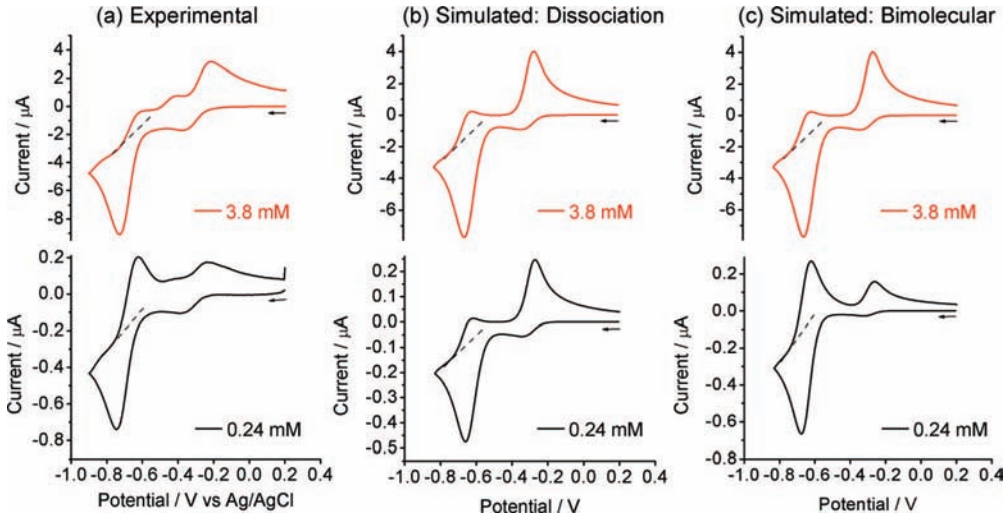


***Figure 6.*** Experimental CVs generated at 0.5 V $s^{-1}$ (baseline subtracted) for (a) 3.8 and 0.24 mM and the corresponding simulated CVs based on the (b) dissociation and (c) bimolecular pathways.

**[2]PR**$^0$. When using 0.5 equiv of a strong reductant a maximum rate would be predicted to occur if $K_E \gg 1$.

## Conclusions

The electrochemical reduction of the tetrazine-based redox-active ligand and the high lability of Cu(I) provide the means to create a reversible supramolecular switch that exchanges between two- and three-component pseudorotaxanes. The [2]- and [3]pseudorotaxanes were formed, respectively, from 1:1 and 2:1 molar ratios of the copper-macrocycle and the 3,6-bis(5-methyl-2-pyridine)-1,2,4,5-tetrazine bridging ligand in sequential steps consistent with $K_1 = 8.9 \times 10^8$ $M^{-1}$ and $K_2 = 3.1 \times 10^6$ $M^{-1}$. The scan-rate dependence of **[2]PR**$^+$ indicates that the generation of 0.5 equiv of a ligand-centered anion provides the electrostatic driving force (−8.4 kcal $mol^{-1}$ = 365 mV) to overcome the negative cooperativity (+3.3 kcal $mol^{-1}$) to form the reduced [3]pseudorotaxane **[3]PR**$^+$ (−5.1 kcal $mol^{-1}$). The stoichiometry of the switching event (2**[2]PR**$^+$ + $e^-$ → **[3]PR**$^+$ + **$Me_2$BPTZ**) and its chemical reversibility was verified using in situ UV−vis−NIR spectroscopic measurements of the electrochemically reduced solution. The concentration dependence of the CVs and their digital simulations provided a means to verify that the reduced **[3]PR**$^+$ is generated by a bimolecular reaction between reduced **[2]PR**$^0$ and unreduced **[2]PR**$^+$ with a second-order rate constant of $k_d = 12\,000$ $s^{-1}$ $M^{-1}$. This proof-of-principle demonstration opens up the possibility to develop new classes of Cu(I) molecular machines on the basis of ligand reductions.

**Acknowledgment.** We acknowledge the experimental aid of Michael Stewart and William E. Geiger at the University of Vermont, and financial support from the National Science Foundation: ECCS-0708582 (AHF), Research Corporation (DVG), and ACS-PRF (DVG). ChemMatCARS Sector 15 for X-ray diffraction experiments is principally supported by the National Science Foundation/Department of Energy under grant number CHE-0535644. Use of the Advanced Photon Source was supported by the U.S. Department of Energy, Office of Science, Office of Basic Energy Sciences, under Contract No. DE-AC02-06CH11357.

**Supporting Information Available:** Syntheses, experimental procedures, modeling, tables of X-ray crystallography, UV−vis−NIR and electrochemistry data, and electrochemical studies. This material is available free of charge via the Internet at http://pubs.acs.org.

JA8085593